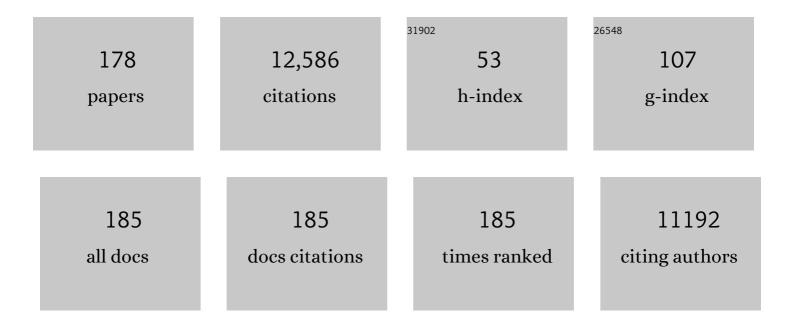
List of Publications by Year in descending order

Source: https://exaly.com/author-pdf/8135893/publications.pdf Version: 2024-02-01



#	Article	IF	CITATIONS
1	Quartz crystal microbalance setup for frequency and Qâ€factor measurements in gaseous and liquid environments. Review of Scientific Instruments, 1995, 66, 3924-3930.	0.6	1,164
2	Variations in Coupled Water, Viscoelastic Properties, and Film Thickness of a Mefp-1 Protein Film during Adsorption and Cross-Linking:Â A Quartz Crystal Microbalance with Dissipation Monitoring, Ellipsometry, and Surface Plasmon Resonance Study. Analytical Chemistry, 2001, 73, 5796-5804.	3.2	1,087
3	Intact Vesicle Adsorption and Supported Biomembrane Formation from Vesicles in Solution:Â Influence of Surface Chemistry, Vesicle Size, Temperature, and Osmotic Pressureâ€. Langmuir, 2003, 19, 1681-1691.	1.6	573
4	Quartz crystal microbalance with dissipation monitoring of supported lipid bilayers on various substrates. Nature Protocols, 2010, 5, 1096-1106.	5.5	471
5	QCM Operation in Liquids:Â An Explanation of Measured Variations in Frequency andQFactor with Liquid Conductivity. Analytical Chemistry, 1996, 68, 2219-2227.	3.2	319
6	Improving the Instrumental Resolution of Sensors Based on Localized Surface Plasmon Resonance. Analytical Chemistry, 2006, 78, 4416-4423.	3.2	305
7	Characterization of DNA Immobilization and Subsequent Hybridization on a 2D Arrangement of Streptavidin on a Biotin-Modified Lipid Bilayer Supported on SiO2. Analytical Chemistry, 2003, 75, 5080-5087.	3.2	292
8	Protein Adsorption on Supported Phospholipid Bilayers. Journal of Colloid and Interface Science, 2002, 246, 40-47.	5.0	282
9	Localized Surface Plasmon Resonance Sensing of Lipid-Membrane-Mediated Biorecognition Events. Journal of the American Chemical Society, 2005, 127, 5043-5048.	6.6	272
10	Simultaneous Surface Plasmon Resonance and Quartz Crystal Microbalance with Dissipation Monitoring Measurements of Biomolecular Adsorption Events Involving Structural Transformations and Variations in Coupled Water. Analytical Chemistry, 2004, 76, 7211-7220.	3.2	271
11	Label-Free Plasmonic Detection of Biomolecular Binding by a Single Gold Nanorod. Analytical Chemistry, 2008, 80, 984-989.	3.2	271
12	DNA-Induced Programmable Fusion of Phospholipid Vesicles. Journal of the American Chemical Society, 2007, 129, 9584-9585.	6.6	267
13	Vesicle adsorption on SiO2 and TiO2: Dependence on vesicle size. Journal of Chemical Physics, 2002, 117, 7401-7404.	1.2	251
14	Plasmonic Sensing Characteristics of Single Nanometric Holes. Nano Letters, 2005, 5, 2335-2339.	4.5	248
15	Bivalent Cholesterol-Based Coupling of Oligonucletides to Lipid Membrane Assemblies. Journal of the American Chemical Society, 2004, 126, 10224-10225.	6.6	238
16	A Method Improving the Accuracy of Fluorescence Recovery after Photobleaching Analysis. Biophysical Journal, 2008, 95, 5334-5348.	0.2	204
17	Strongly Stretched Protein Resistant Poly(ethylene glycol) Brushes Prepared by Grafting-To. ACS Applied Materials & Interfaces, 2015, 7, 7505-7515.	4.0	142
18	High-Performance Biosensing Using Arrays of Plasmonic Nanotubes. ACS Nano, 2010, 4, 2210-2216.	7.3	140

#	Article	IF	CITATIONS
19	Supported Lipid Bilayer Formation and Lipid-Membrane-Mediated Biorecognition Reactions Studied with a New Nanoplasmonic Sensor Template. Nano Letters, 2007, 7, 3462-3468.	4.5	139
20	Determination of Exosome Concentration in Solution Using Surface Plasmon Resonance Spectroscopy. Analytical Chemistry, 2014, 86, 5929-5936.	3.2	133
21	Patterns of DNA-Labeled and scFv-Antibody-Carrying Lipid Vesicles Directed by Material-Specific Immobilization of DNA and Supported Lipid Bilayer Formation on an Au/SiO2 Template. ChemBioChem, 2003, 4, 339-343.	1.3	132
22	Measurements Using the Quartz Crystal Microbalance Technique of Ferritin Monolayers on Methyl-Thiolated Gold: Dependence of Energy Dissipation and Saturation Coverage on Salt Concentration. Journal of Colloid and Interface Science, 1998, 208, 63-67.	5.0	124
23	Determinants for Membrane Fusion Induced by Cholesterol-Modified DNA Zippers. Journal of Physical Chemistry B, 2008, 112, 8264-8274.	1.2	112
24	Improving the Limit of Detection of Nanoscale Sensors by Directed Binding to High-Sensitivity Areas. ACS Nano, 2010, 4, 2167-2177.	7.3	112
25	Formation of Supported Lipid Bilayer Membranes on SiO2from Proteoliposomes Containing Transmembrane Proteins. Langmuir, 2003, 19, 842-850.	1.6	107
26	Locally Functionalized Short-Range Ordered Nanoplasmonic Pores for Bioanalytical Sensing. Analytical Chemistry, 2010, 82, 2087-2094.	3.2	105
27	Surface-Based Gold-Nanoparticle Sensor for Specific and Quantitative DNA Hybridization Detection. Langmuir, 2003, 19, 10414-10419.	1.6	103
28	Comparison of surface plasmon resonance and quartz crystal microbalance in the study of whole blood and plasma coagulation. Biosensors and Bioelectronics, 2000, 15, 605-613.	5.3	98
29	Single-Molecule Detection and Mismatch Discrimination of Unlabeled DNA Targets. Nano Letters, 2008, 8, 183-188.	4.5	95
30	Single-molecule biosensors: Recent advances and applications. Biosensors and Bioelectronics, 2020, 151, 111944.	5.3	95
31	Influence of the Evanescent Field Decay Length on the Sensitivity of Plasmonic Nanodisks and Nanoholes. ACS Photonics, 2015, 2, 256-262.	3.2	94
32	A Dual-Frequency QCM-D Setup Operating at Elevated Oscillation Amplitudes. Analytical Chemistry, 2005, 77, 4918-4926.	3.2	93
33	Micropatterning of DNA-Tagged Vesicles. Langmuir, 2004, 20, 11348-11354.	1.6	89
34	Design of Surface Modifications for Nanoscale Sensor Applications. Sensors, 2015, 15, 1635-1675.	2.1	88
35	Mucosal Vaccine Development Based on Liposome Technology. Journal of Immunology Research, 2016, 2016, 1-16.	0.9	84
36	Promises and challenges of nanoplasmonic devices for refractometric biosensing. Nanophotonics, 2013, 2, 83-101.	2.9	83

#	Article	IF	CITATIONS
37	High-Resolution Microspectroscopy of Plasmonic Nanostructures for Miniaturized Biosensing. Analytical Chemistry, 2009, 81, 6572-6580.	3.2	80
38	Individual Nanometer Hole–Particle Pairs for Surfaceâ€Enhanced Raman Scattering. Small, 2008, 4, 1296-1300.	5.2	78
39	Adsorption behavior and enzymatically or chemically induced crossâ€linking of a mussel adhesive protein. Biofouling, 2000, 16, 119-132.	0.8	77
40	Simultaneous Nanoplasmonic and Quartz Crystal Microbalance Sensing: Analysis of Biomolecular Conformational Changes and Quantification of the Bound Molecular Mass. Analytical Chemistry, 2008, 80, 7988-7995.	3.2	77
41	Preserved Transmembrane Protein Mobility in Polymer-Supported Lipid Bilayers Derived from Cell Membranes. Analytical Chemistry, 2015, 87, 9194-9203.	3.2	74
42	DNA-Based Formation of a Supported, Three-Dimensional Lipid Vesicle Matrix Probed by QCM-D and SPR. ChemPhysChem, 2004, 5, 729-733.	1.0	72
43	Measurement of the Dynamics of Exocytosis and Vesicle Retrieval at Cell Populations Using a Quartz Crystal Microbalance. Analytical Chemistry, 2001, 73, 5805-5811.	3.2	70
44	Dual-Wavelength Surface Plasmon Resonance for Determining the Size and Concentration of Sub-Populations of Extracellular Vesicles. Analytical Chemistry, 2016, 88, 9980-9988.	3.2	70
45	Nanoplasmonic biosensing with focus on short-range ordered nanoholes in thin metal films (Review). Biointerphases, 2008, 3, FD30-FD40.	0.6	66
46	Material-Selective Surface Chemistry for Nanoplasmonic Sensors: Optimizing Sensitivity and Controlling Binding to Local Hot Spots. Nano Letters, 2012, 12, 873-879.	4.5	65
47	Evanescent Light-Scattering Microscopy for Label-Free Interfacial Imaging: From Single Sub-100 nm Vesicles to Live Cells. ACS Nano, 2015, 9, 11849-11862.	7.3	65
48	Use of PLL-g-PEG in Micro-Fluidic Devices for Localizing Selective and Specific Protein Binding. Langmuir, 2006, 22, 10103-10108.	1.6	62
49	Specific Selfâ€Assembly of Single Lipid Vesicles in Nanoplasmonic Apertures in Gold. Advanced Materials, 2008, 20, 1436-1442.	11.1	61
50	Synchronized Quartz Crystal Microbalance and Nanoplasmonic Sensing of Biomolecular Recognition Reactions. ACS Nano, 2008, 2, 2174-2182.	7.3	61
51	Viscoelastic Modeling of Template-Directed DNA Synthesis. Analytical Chemistry, 2005, 77, 3709-3714.	3.2	60
52	Rupture Pathway of Phosphatidylcholine Liposomes on Silicon Dioxide. International Journal of Molecular Sciences, 2009, 10, 1683-1696.	1.8	60
53	Quantification of Multivalent Interactions by Tracking Single Biological Nanoparticle Mobility on a Lipid Membrane. Nano Letters, 2016, 16, 4382-4390.	4.5	58
54	Adsorption of cubic liquid crystalline nanoparticles on model membranes. Soft Matter, 2008, 4, 2267.	1.2	56

#	Article	IF	CITATIONS
55	Single Vesicle Analysis Reveals Nanoscale Membrane Curvature Selective Pore Formation in Lipid Membranes by an Antiviral α-Helical Peptide. Nano Letters, 2012, 12, 5719-5725.	4.5	56
56	Bivalent-Ion-Mediated Vesicle Adsorption and Controlled Supported Phospholipid Bilayer Formation on Molecular Phosphate and Sulfate Layers on Gold. Langmuir, 2002, 18, 7923-7929.	1.6	54
57	Shear-Driven Motion of Supported Lipid Bilayers in Microfluidic Channels. Journal of the American Chemical Society, 2009, 131, 5294-5297.	6.6	54
58	QCM-D studies of human norovirus VLPs binding to glycosphingolipids in supported lipid bilayers reveal strain-specific characteristics. Glycobiology, 2009, 19, 1176-1184.	1.3	53
59	DNA Binding to Zwitterionic Model Membranes. Langmuir, 2010, 26, 4965-4976.	1.6	49
60	Single-vesicle imaging reveals lipid-selective and stepwise membrane disruption by monomeric α-synuclein. Proceedings of the National Academy of Sciences of the United States of America, 2020, 117, 14178-14186.	3.3	49
61	Mechanical Behavior of a Supported Lipid Bilayer under External Shear Forces. Langmuir, 2009, 25, 6279-6286.	1.6	47
62	Liposome-Based Chemical Barcodes for Single Molecule DNA Detection Using Imaging Mass Spectrometry. Nano Letters, 2010, 10, 732-737.	4.5	46
63	The Influence of Cross-Linking on Proteinâ <sup>~,</sup> 'Protein Interactions in a Marine Adhesive:Â The Case of Two Byssus Plaque Proteins from the Blue Mussel. Biomacromolecules, 2002, 3, 732-741.	2.6	45
64	Alpha-Helical Peptide-Induced Vesicle Rupture Revealing New Insight into the Vesicle Fusion Process As Monitored <i>in Situ</i> by Quartz Crystal Microbalance-Dissipation and Reflectometry. Analytical Chemistry, 2009, 81, 4752-4761.	3.2	45
65	Heavy Meromyosin Molecules Extending More Than 50 nm above Adsorbing Electronegative Surfaces. Langmuir, 2010, 26, 9927-9936.	1.6	43
66	Sealing of Submicrometer Wells by a Shear-Driven Lipid Bilayer. Nano Letters, 2010, 10, 1900-1906.	4.5	42
67	Spatial-Resolution Limits in Mass Spectrometry Imaging of Supported Lipid Bilayers and Individual Lipid Vesicles. Analytical Chemistry, 2010, 82, 2426-2433.	3.2	42
68	Structural Effects in the Analysis of Supported Lipid Bilayers by Time-of-Flight Secondary Ion Mass Spectrometry. Langmuir, 2007, 23, 8035-8041.	1.6	41
69	Accumulation and Separation of Membrane-Bound Proteins Using Hydrodynamic Forces. Analytical Chemistry, 2011, 83, 604-611.	3.2	41
70	Adsorption of a small protein to a methyl-terminated hydrophobic surfaces: effect of protein-folding thermodynamics and kinetics. Colloids and Surfaces B: Biointerfaces, 2003, 29, 67-73.	2.5	40
71	Generic surface modification strategy for sensing applications based on Au/SiO2 nanostructures. Biointerphases, 2007, 2, 49-55.	0.6	40
72	Self-assembly formation of multiple DNA-tethered lipid bilayers. Journal of Structural Biology, 2009, 168, 200-206.	1.3	39

#	Article	IF	CITATIONS
73	Phase transitions in adsorbed lipid vesicles measured using a quartz crystal microbalance with dissipation monitoring. Soft Matter, 2011, 7, 10749.	1.2	39
74	Plasmonic Nanopores in Metalâ€Insulatorâ€Metal Films. Advanced Optical Materials, 2014, 2, 556-564.	3.6	38
75	Gravimetric antigen detection utilizing antibody-modified lipid bilayers. Analytical Biochemistry, 2005, 345, 72-80.	1.1	37
76	Nanoplasmonic biosensing with on-chip electrical detection. Biosensors and Bioelectronics, 2010, 26, 1131-1136.	5.3	37
77	Simultaneous Imaging of Amyloid-β and Lipids in Brain Tissue Using Antibody-Coupled Liposomes and Time-of-Flight Secondary Ion Mass Spectrometry. Journal of the American Chemical Society, 2014, 136, 9973-9981.	6.6	37
78	Conformation of Human Carbonic Anhydrase II Variants Adsorbed to Silica Nanoparticles. Langmuir, 1999, 15, 6395-6399.	1.6	35
79	Refractive-Index-Based Screening of Membrane-Protein-Mediated Transfer across Biological Membranes. Biophysical Journal, 2010, 99, 124-133.	0.2	35
80	MicroRNA Detection by DNAâ€Mediated Liposome Fusion. ChemBioChem, 2018, 19, 434-438.	1.3	35
81	Two-dimensional flow nanometry of biological nanoparticles for accurate determination of their size and emission intensity. Nature Communications, 2016, 7, 12956.	5.8	34
82	Pentacyclic adenine: a versatile and exceptionally bright fluorescent DNA base analogue. Chemical Science, 2018, 9, 3494-3502.	3.7	34
83	Site‣pecific DNAâ€Controlled Fusion of Single Lipid Vesicles to Supported Lipid Bilayers. ChemPhysChem, 2010, 11, 1011-1017.	1.0	33
84	Continuous Lipid Bilayers Derived from Cell Membranes for Spatial Molecular Manipulation. Journal of the American Chemical Society, 2011, 133, 14027-14032.	6.6	33
85	Size and Refractive Index Determination of Subwavelength Particles and Air Bubbles by Holographic Nanoparticle Tracking Analysis. Analytical Chemistry, 2020, 92, 1908-1915.	3.2	32
86	Norovirus GII.4 Virusâ€like Particles Recognize Galactosylceramides in Domains of Planar Supported Lipid Bilayers. Angewandte Chemie - International Edition, 2012, 51, 12020-12024.	7.2	31
87	Single Lipid Vesicle Assay for Characterizing Single-Enzyme Kinetics of Phospholipid Hydrolysis in a Complex Biological Fluid. Journal of the American Chemical Society, 2013, 135, 14151-14158.	6.6	30
88	Kinetic and thermodynamic characterization of single-mismatch discrimination using single-molecule imaging. Nucleic Acids Research, 2009, 37, e99-e99.	6.5	29
89	Fast and Accurate Nanoparticle Characterization Using Deep-Learning-Enhanced Off-Axis Holography. ACS Nano, 2021, 15, 2240-2250.	7.3	28
90	Separation of Bulk Effects and Bound Mass during Adsorption of Surfactants Probed by Quartz Crystal Microbalance with Dissipation: Insight into Data Interpretation. Analytical Chemistry, 2010, 82, 9116-9121	3.2	27

#	Article	IF	CITATIONS
91	Kinetics of Ligand Binding to Membrane Receptors from Equilibrium Fluctuation Analysis of Single Binding Events. Journal of the American Chemical Society, 2011, 133, 14852-14855.	6.6	27
92	Investigation of binding event perturbations caused by elevated QCM-D oscillation amplitude. Analyst, The, 2006, 131, 822-828.	1.7	26
93	Hydrogels from a Water-Soluble Zwitterionic Polythiophene:Â Dynamics under pH Change and Biomolecular Interactions Observed Using Quartz Crystal Microbalance with Dissipation Monitoring. Langmuir, 2005, 21, 7292-7298.	1.6	25
94	Equilibrium-fluctuation-analysis of single liposome binding events reveals how cholesterol and Ca2+ modulate glycosphingolipid trans-interactions. Scientific Reports, 2013, 3, 1452.	1.6	25
95	Label-free spatio-temporal monitoring of cytosolic mass, osmolarity, and volume in living cells. Nature Communications, 2019, 10, 340.	5.8	25
96	Influence of Bile Composition on Membrane Incorporation of Transient Permeability Enhancers. Molecular Pharmaceutics, 2020, 17, 4226-4240.	2.3	24
97	Enhancing the Cellular Uptake and Antibacterial Activity of Rifampicin through Encapsulation in Mesoporous Silica Nanoparticles. Nanomaterials, 2020, 10, 815.	1.9	24
98	Supported lipid bilayers, tethered lipid vesicles, and vesicle fusion investigated using gravimetric, plasmonic, and microscopy techniques. Biointerphases, 2008, 3, FA108-FA116.	0.6	23
99	Neutralized Chimeric Avidin Binding at a Reference Biosensor Surface. Langmuir, 2015, 31, 1921-1930.	1.6	23
100	Drug Discovery at the Single Molecule Level: Inhibition-in-Solution Assay of Membrane-Reconstituted β-Secretase Using Single-Molecule Imaging. Analytical Chemistry, 2015, 87, 4100-4103.	3.2	23
101	Nanomaterial interactions with biomembranes: Bridging the gap between soft matter models and biological context. Biointerphases, 2018, 13, 028501.	0.6	23
102	Simultaneous, Single-Particle Measurements of Size and Loading Give Insights into the Structure of Drug-Delivery Nanoparticles. ACS Nano, 2021, 15, 19244-19255.	7.3	23
103	Quantification of Oligonucleotide Modifications of Small Unilamellar Lipid Vesicles. Analytical Chemistry, 2006, 78, 7493-7498.	3.2	22
104	Investigation of Adsorption and Cross-Linking of a Mussel Adhesive Protein Using Attenuated Total Internal Reflection Fourier Transform Infrared Spectroscopy (ATR-FTIR). Journal of Adhesion, 2010, 86, 25-38.	1.8	22
105	Histo-Blood Group Antigen Presentation Is Critical for Binding of Norovirus VLP to Glycosphingolipids in Model Membranes. ACS Chemical Biology, 2017, 12, 1288-1296.	1.6	22
106	Protein-Containing Lipid Bilayers Intercalated with Size-Matched Mesoporous Silica Thin Films. Nano Letters, 2017, 17, 476-485.	4.5	22
107	Effective Refractive Index and Lipid Content of Extracellular Vesicles Revealed Using Optical Waveguide Scattering and Fluorescence Microscopy. Langmuir, 2018, 34, 8522-8531.	1.6	22
108	A vaccine combination of lipid nanoparticles and a cholera toxin adjuvant derivative greatly improves lung protection against influenza virus infection. Mucosal Immunology, 2021, 14, 523-536.	2.7	22

#	Article	IF	CITATIONS
109	Labelâ€Free Measurements of Molecular Transport across Liposome Membranes using Evanescentâ€Wave Sensing. ChemPhysChem, 2008, 9, 2480-2485.	1.0	21
110	Total internal reflection fluorescence microscopy for determination of size of individual immobilized vesicles: Theory and experiment. Journal of Applied Physics, 2015, 118, .	1.1	21
111	Nonspecific Colloidal-Type Interaction Explains Size-Dependent Specific Binding of Membrane-Targeted Nanoparticles. ACS Nano, 2016, 10, 9974-9982.	7.3	21
112	Hydrolysis of a Lipid Membrane by Single Enzyme Molecules: Accurate Determination of Kinetic Parameters. Angewandte Chemie - International Edition, 2015, 54, 1022-1026.	7.2	20
113	Assembly of RNA nanostructures on supported lipid bilayers. Nanoscale, 2015, 7, 583-596.	2.8	20
114	Structure and Composition of Native Membrane Derived Polymer-Supported Lipid Bilayers. Analytical Chemistry, 2018, 90, 13065-13072.	3.2	20
115	Spatiotemporal Kinetics of Supported Lipid Bilayer Formation on Glass via Vesicle Adsorption and Rupture. Journal of Physical Chemistry Letters, 2018, 9, 5143-5149.	2.1	20
116	Quantitative interpretation of gold nanoparticle-based bioassays designed for detection of immunocomplex formation. Biointerphases, 2007, 2, 6-15.	0.6	19
117	Kinetics of the enzyme–vesicle interaction including the formation of rafts and membrane strain. Biophysical Chemistry, 2012, 170, 17-24.	1.5	19
118	Formation and Diffusivity Characterization of Supported Lipid Bilayers with Complex Lipid Compositions. Langmuir, 2012, 28, 10528-10533.	1.6	19
119	Molecular motors on lipid bilayers and silicon dioxide: different driving forces for adsorption. Soft Matter, 2010, 6, 3211.	1.2	18
120	Interaction of Virus-Like Particles with Vesicles Containing Glycolipids: Kinetics of Detachment. Journal of Physical Chemistry B, 2015, 119, 11466-11472.	1.2	18
121	Detachment of Membrane Bound Virions by Competitive Ligand Binding Induced Receptor Depletion. Langmuir, 2017, 33, 4049-4056.	1.6	18
122	Competition for Membrane Receptors: Norovirus Detachment via Lectin Attachment. Journal of the American Chemical Society, 2019, 141, 16303-16311.	6.6	18
123	Hybrid vesicles as intracellular reactive oxygen species and nitric oxide generators. Nanoscale, 2019, 11, 11530-11541.	2.8	18
124	Characterization of a proton pumping transmembrane protein incorporated into a supported three-dimensional matrix of proteoliposomes. Analytical Biochemistry, 2007, 367, 87-94.	1.1	17
125	Light-regulated release of liposomes from phospholipid membranes via photoresponsive polymer–DNA conjugates. Soft Matter, 2006, 2, 710-715.	1.2	16
126	A functioning artificial secretory cell. Scientific Reports, 2012, 2, 824.	1.6	16

#	Article	IF	CITATIONS
127	High throughput fabrication of plasmonic nanostructures in nanofluidic pores for biosensing applications. Nanotechnology, 2012, 23, 415304.	1.3	15
128	Solute transport on the sub 100 ms scale across the lipid bilayer membrane of individual proteoliposomes. Lab on A Chip, 2012, 12, 4635.	3.1	15
129	Imaging of amyloid-β in Alzheimer's disease transgenic mouse brains with ToF-SIMS using immunoliposomes. Biointerphases, 2016, 11, 02A312.	0.6	15
130	Versailles project on advanced materials and standards (VAMAS) interlaboratory study on measuring the number concentration of colloidal gold nanoparticles. Nanoscale, 2022, 14, 4690-4704.	2.8	15
131	Time-Resolved Surface-Enhanced Ellipsometric Contrast Imaging for Label-Free Analysis of Biomolecular Recognition Reactions on Glycolipid Domains. Analytical Chemistry, 2012, 84, 6538-6545.	3.2	14
132	A virus biosensor with single virus-particle sensitivity based on fluorescent vesicle labels and equilibrium fluctuation analysis. Biointerphases, 2013, 8, 4.	0.6	14
133	Supported lipid bilayer repair mediated by AH peptide. Physical Chemistry Chemical Physics, 2016, 18, 3040-3047.	1.3	14
134	Utilizing adsorbed proteoliposomes trapped in a non-ruptured state on SiO2 for amplified detection of membrane proteins. Biosensors and Bioelectronics, 2004, 20, 498-504.	5.3	13
135	Resonance-Mode Electrochemical Impedance Measurements of Silicon Dioxide Supported Lipid Bilayer Formation and Ion Channel Mediated Charge Transport. Analytical Chemistry, 2011, 83, 7800-7806.	3.2	13
136	Labelâ€Free Measurements of the Diffusivity of Molecules in Lipid Membranes. ChemPhysChem, 2014, 15, 486-491.	1.0	12
137	Hydrodynamic Propulsion of Liposomes Electrostatically Attracted to a Lipid Membrane Reveals Size-Dependent Conformational Changes. ACS Nano, 2016, 10, 8812-8820.	7.3	12
138	Membrane Deformation Induces Clustering of Norovirus Bound to Glycosphingolipids in a Supported Cell-Membrane Mimic. Journal of Physical Chemistry Letters, 2018, 9, 2278-2284.	2.1	12
139	Affinity Purification and Single-Molecule Analysis of Integral Membrane Proteins from Crude Cell-Membrane Preparations. Nano Letters, 2018, 18, 381-385.	4.5	12
140	Bioinspired, nanoscale approaches in contemporary bioanalytics (Review). Biointerphases, 2018, 13, 040801.	0.6	12
141	Addressable adsorption of lipid vesicles and subsequent protein interaction studies. Biointerphases, 2008, 3, 29-37.	0.6	11
142	Single Proteoliposomes with <i>E.Âcoli</i> Quinol Oxidase: Proton Pumping without Transmembrane Leaks. Israel Journal of Chemistry, 2017, 57, 437-445.	1.0	11
143	Single-Molecule Detection with Lightguiding Nanowires: Determination of Protein Concentration and Diffusivity in Supported Lipid Bilayers. Nano Letters, 2019, 19, 6182-6191.	4.5	11
144	Control of Polymer Brush Morphology, Rheology, and Protein Repulsion by Hydrogen Bond Complexation. Langmuir, 2021, 37, 4943-4952.	1.6	11

#	Article	IF	CITATIONS
145	Physicochemical tools for studying virus interactions with targeted cell membranes in a molecular and spatiotemporally resolved context. Analytical and Bioanalytical Chemistry, 2021, 413, 7157-7178.	1.9	11
146	Diffusion-limited attachment of large spherical particles to flexible membrane-immobilized receptors. European Biophysics Journal, 2015, 44, 219-226.	1.2	10
147	Plasmon-enhanced four-wave mixing by nanoholes in thin gold films. Optics Letters, 2014, 39, 1001.	1.7	9
148	Time-Resolved and Label-Free Evanescent Light-Scattering Microscopy for Mass Quantification of Protein Binding to Single Lipid Vesicles. Nano Letters, 2021, 21, 4622-4628.	4.5	9
149	Determination of Nanosized Adsorbate Mass in Solution Using Mechanical Resonators: Elimination of the So Far Inseparable Liquid Contribution. Journal of Physical Chemistry C, 2021, 125, 22733-22746.	1.5	9
150	Controlled Radial Distribution of Nanoscale Vesicles During Binding to an Oscillating QCM Surface. Small, 2007, 3, 585-589.	5.2	8
151	Effects of Surface Pressure and Internal Friction on the Dynamics of Shear-Driven Supported Lipid Bilayers. Langmuir, 2011, 27, 1430-1439.	1.6	8
152	Equilibrium-Fluctuation Analysis for Interaction Studies between Natural Ligands and Single G Protein-Coupled Receptors in Native Lipid Vesicles. Langmuir, 2015, 31, 10774-10780.	1.6	8
153	Fluorescence Signal Enhancement in Antibody Microarrays Using Lightguiding Nanowires. Nanomaterials, 2021, 11, 227.	1.9	8
154	Investigation of Self-Emulsifying Drug-Delivery System Interaction with a Biomimetic Membrane under Conditions Relevant to the Small Intestine. Langmuir, 2021, 37, 10200-10213.	1.6	8
155	Low-temperature fabrication and characterization of a symmetric hybrid organic–inorganic slab waveguide for evanescent light microscopy. Nano Futures, 2018, 2, 025007.	1.0	7
156	Gel Phase 1,2-Distearoyl-sn-glycero-3-phosphocholine-Based Liposomes Are Superior to Fluid Phase Liposomes at Augmenting Both Antigen Presentation on Major Histocompatibility Complex Class II and Costimulatory Molecule Display by Dendritic Cells in Vitro. ACS Infectious Diseases, 2019, 5, 1867-1878.	1.8	7
157	Charged Polystyrene Nanoparticles Near a SiO <sub>2</sub> /Water Interface. Langmuir, 2019, 35, 222-228.	1.6	7
158	TIRF Microscopyâ€Based Monitoring of Drug Permeation Across a Lipid Membrane Supported on Mesoporous Silica. Angewandte Chemie - International Edition, 2021, 60, 2069-2073.	7.2	7
159	Dissimilar Deformation of Fluid- and Gel-Phase Liposomes upon Multivalent Interaction with Cell Membrane Mimics Revealed Using Dual-Wavelength Surface Plasmon Resonance. Langmuir, 2022, 38, 2550-2560.	1.6	7
160	Nanoplasmonic Sensing Combined with Artificial Cell Membranes. , 2012, , 59-82.		6
161	Affinity Capturing and Surface Enrichment of a Membrane Protein Embedded in a Continuous Supported Lipid Bilayer. ChemistryOpen, 2016, 5, 445-449.	0.9	6
162	Sticking particles to solid surfaces using Moringa oleifera proteins as a glue. Colloids and Surfaces B: Biointerfaces, 2018, 168, 68-75.	2.5	6

#	Article	IF	CITATIONS
163	Avidity-Based Affinity Enhancement Using Nanoliposome-Amplified SPR Sensing Enables Low Picomolar Detection of Biologically Active Neuregulin 1. ACS Sensors, 2019, 4, 3166-3174.	4.0	6
164	Independent Size and Fluorescence Emission Determination of Individual Biological Nanoparticles Reveals that Lipophilic Dye Incorporation Does Not Scale with Particle Size. Langmuir, 2020, 36, 9693-9700.	1.6	6
165	TIRF Microscopyâ€Based Monitoring of Drug Permeation Across a Lipid Membrane Supported on Mesoporous Silica. Angewandte Chemie, 2021, 133, 2097-2101.	1.6	6
166	Formation of Supported Lipid Bilayers Derived from Vesicles of Various Compositional Complexity on Conducting Polymer/Silica Substrates. Langmuir, 2021, 37, 5494-5505.	1.6	6
167	Hydrodynamic separation of proteins in supported lipid bilayers confined by gold barriers. Soft Matter, 2013, 9, 9414.	1.2	5
168	Diffusion of Lipid Nanovesicles Bound to a Lipid Membrane Is Associated with the Partial-Slip Boundary Condition. Nano Letters, 2021, 21, 8503-8509.	4.5	5
169	Suppression of binding events via external perturbation with emphasis on QCM. Chemical Physics Letters, 2006, 424, 214-217.	1.2	4
170	Nanometer-scale molecular organization in lipid membranes studied by time-of-flight secondary ion mass spectrometry. Biointerphases, 2018, 13, 03B408.	0.6	4
171	Toward multiplexed quantification of biomolecules on surfaces using time-of-flight secondary ion mass spectrometry. Biointerphases, 2018, 13, 03B413.	0.6	4
172	Antenna-Enhanced Fluorescence Correlation Spectroscopy Resolves Calcium-Mediated Lipid–Lipid Interactions. ACS Nano, 2018, 12, 3272-3279.	7.3	3
173	Enhanced Optical Biosensing by Aerotaxy Ga(As)P Nanowire Platforms Suitable for Scalable Production. ACS Applied Nano Materials, 0, , .	2.4	3
174	Simulation of dissociation of DNA duplexes attached to the surface. Open Physics, 2010, 8, .	0.8	2
175	Inside Cover: Site-Specific DNA-Controlled Fusion of Single Lipid Vesicles to Supported Lipid Bilayers (ChemPhysChem 5/2010). ChemPhysChem, 2010, 11, 926-926.	1.0	1
176	Kinetics of enzyme-mediated hydrolysis of lipid vesicles. Chemical Physics Letters, 2016, 663, 51-56.	1.2	1
177	Quantitative Detection of Biological Nanoparticles in Solution via Their Mediation of Colocalization of Fluorescent Liposomes. Physical Review Applied, 2019, 12, .	1.5	1
178	2014, 2, 555-555.	3.6	0